Defense Technical Information Center
Compilation Part Notice

ADP013772

TITLE: Size Effects in Epitaxial Films of Magnetite

DISTRIBUTION: Approved for public release, distribution unlimited

This paper is part of the following report:

TITLE: THIN SOLID FILMS: An International Journal on the Science and Technology of Condensed Matter Films. Volume 412 Nos. 1-2, June 3, 2002. Proceedings of the Workshop on MBE and VPE Growth, Physics, Technology [4th], Held in Warsaw, Poland, on 24-28 September 2001

To order the complete compilation report, use: ADA412911

The component part is provided here to allow users access to individually authored sections of proceedings, annals, symposia, etc. However, the component should be considered within the context of the overall compilation report and not as a stand-alone technical report.

The following component part numbers comprise the compilation report:
ADP013771 thru ADP013789

Size effects in epitaxial films of magnetite

J. Korecki[a,b,*], B. Handke[a,b], N. Spiridis[a], T. Ślęzak[b], I. Flis-Kabulska[c], J. Haber[a]

[a]*Institute of Catalysis and Surface Chemistry, Polish Academy of Sciences, Niezapominajek 8, 30-239 Kraków, Poland*
[b]*Faculty of Physics and Nuclear Techniques, University of Mining and Metallurgy, Al. Mickiewicza 30, 30-059 Kraków, Poland*
[c]*Institute of Physical Chemistry, Polish Academy of Sciences, Kasprzaka 44/52, 01-224 Warszawa, Poland*

Abstract

Resent results concerning epitaxial $Fe_3O_4(001)$ films grown by reactive deposition on $MgO(001)$ substrates as well as obtained by oxidation of epitaxial $Fe(001)$ films are reviewed. Conversion electron Mössbauer spectroscopy (CEMS) performed in and ex situ was used to check the stoichiometry and electronic properties with monolayer resolution. Size effects were reflected in reduction of the Verwey temperature for the film thickness less than 50 nm. With further decrease in thickness, the films showed strong deviation from the bulk properties due to formation of a magnesium rich phase near the MgO/Fe_3O_4 interface. Surface oxidation to $\gamma-Fe_2O_3$, which can be reversed by annealing, was found using CEMS. The atomic scale surface characterization was accomplished for the first time in situ by the scanning tunneling microscopy, which revealed details of the surface reconstruction and termination. © 2002 Elsevier Science B.V. All rights reserved.

Keywords: Magnetite; Thin epitaxial films; Conversion electron Mössbauer spectroscopy; Scanning tunneling microscopy; Surface reconstruction

1. Introduction

Transition-metal oxides are a subject of intensive research for their interesting physical phenomenology [1] and technological importance as catalysts [2], anticorrosives [3] and magnetic materials [4]. Magnetite (F_3O_4), as a strongly correlated material, combines the full spin polarization on the Fermi level with a high Curie temperature and has potential industrial application in magnetic recording or spin electronics [5] and also as a catalytic support [6]. Magnetite shows native conductivity, being one of a few exceptions among simple metal oxides and therefore can be easily studied with the scanning tunneling microscopy (STM), a powerful method in the model catalyst studies. The model catalyst studies with oxide materials have often faced numerous problems connected with the preparation of reproducible and well-characterized single crystal surfaces [7]. Difficulties in preparation of that type, reported also for magnetite [8], can be overcome by the thin film technology enabling to grow a high quality Fe_3O_4 surface by the reactive molecular beam epitaxy (MBE).

---
*Corresponding author. Faculty of Physics and Nuclear Techniques, University of Mining and Metallurgy, al. Mickiewicza 30, 30-059 Kraków, Poland. Tel.: +48-12-617-2911; fax: +48-12-634-1247.
E-mail address: korecki@uci.agh.edu.pl (J. Korecki).

Epitaxial magnetite films are also important for spin dependent transport devices, as the mobile electrons may be 100% polarized. However, many features of structural, electronic and magnetic properties of thin films are still under debate [9–11]. Size and surface effects lead to strong deviations from bulk properties, which additionally depend on the sample thickness and stoichiometry varying for different technological parameters of the growth process. Additionally, the stoichiometry and structure of the surface and interface layers may differ from that of the film interior. Few atomic layers forming the phase boundary are often crucial with regard to the phenomena of the interest. This is just the case of the catalytic reactions or tunneling, which are typical surface/interface processes.

Magnetite crystallizes in the cubic inverse spinel structure. The oxygen ions form a closed packed cubic structure with Fe ions localized in two different sites, octahedral and tetrahedral. The tetrahedral sites (A) are occupied by trivalent Fe ions. Tri- and divalent Fe ions occupying the octahedral sites (B) are randomly arranged at room temperature because of an electron hopping. Below $T_V \sim 125$ K the electron hopping ceases and the Fe ion charge undergoes a long range ordering. This leads to a metal–insulator transition known as the Verwey transition. The transition concerns not only

electric properties but can be also seen in the heat capacity [12] or magneto-resistance measurements [13], and has a strong manifestation in the hyperfine interactions probed by the Mössbauer spectroscopy, which has been widely used in bulk magnetite studies [14]. At room temperature, when the electron hopping process is fast, the Mössbauer spectrum is characterized by two sextets. The one with the hyperfine magnetic field $B_{hf} = 48.8$ T and the isomer shift IS $= 0.27$ mm/s relative to α-Fe corresponds to the Fe_A^{3+} ions at the tetrahedral A-sites. The second one with $B_{hf} = 45.7$ T and IS $= 0.65$ mm/s is the $Fe_B^{2.5+}$-like average signal from the cations at the octahedral B sites. Fe_B^{+2} and Fe_B^{3+} are indistinguishable due to a fast electron transfer (electron hopping), which is faster ($\tau \sim 1$ ns) than the ^{57}Fe excited state lifetime (98 ns). The magnetite unit cell contains eight Fe_A^{3+} ions and eight Fe_B^{2+} and Fe_B^{3+} ions, 16 in total at the B sites, therefore, the intensity ratio $\beta = I(B)/I(A)$ of the two spectral components is a sensitive measure of the stoichiometry. Assuming that the room temperature ratio of the recoil-free fractions f_B/f_A for the B and A sites is 0.97 [15], the intensity ratio β for perfect stoichiometry should be 1.94. In non-stoichiometric magnetite, under an excess of oxygen, cation vacancies at the B sites are created. The vacancies screen the charge transfer and isolate the hopping process. For each vacancy, five Fe^{3+} ions in octahedral sites become trapped. In the Mössbauer spectrum these trapped Fe^{3+} ions at the octahedral sites and Fe^{3+} ions at tetrahedral sites are indistinguishable without applying an external magnetic field. Therefore, in the spectrum of non-stoichiometric magnetite, intensity transfer from the $Fe_B^{2.5+}$ to Fe_A^{3+}-like components is observed. Therefore, the intensity ratio β decreases markedly with the oxidation process, until the stoichiometry reaches the γ-Fe_2O_3 phase, which is represented by a single unresolved Zeeman component, close to that characteristic of the Fe_A^{3+} site in magnetite.

Below T_V the Mössbauer spectrum becomes complicated and difficult to interpret, comprising a superposition of at least five components. Any impurities and vacancies screen the hopping process, lowering the transition temperature and changing the character of the transition. The sharp first order Verwey transition in stoichiometric magnetite becomes smoother and more second order-like.

Electronic transport in magnetite is determined by the short-range interactions between the nearest neighbors that are the iron ions in the octahedral sites. Thus, in the case of the systems with reduced dimensionality, a strong influence on the phase transition, coming from the film microstructure and the surface or interface related phenomena, is expected. It is difficult to distinguish between intrinsic size effects and effects related to deviation from the stoichiometry at the interface and surface. In the present paper we discuss Mössbauer

results, which partially solve this problem by an analysis of the surface and interface stoichiometry of thin epitaxial magnetite films.

The conversion electron Mössbauer spectroscopy (CEMS) has numerous advantages when applied to thin films. Contrary to most of the surface sensitive methods, CEMS has an ability to probe buried layers and interfaces with the monolayer sensitivity for films made of a pure Mössbauer isotope [16]. The method gives the atomic scale local characterization of chemical, structural and magnetic properties, simultaneously. The CEMS measurements are ultra high vacuum compatible, which gives the possibility of in situ investigations of clean surfaces in a wide temperature range. Exceptional sensitivity of our CEMS measurements (below one monolayer of ^{57}Fe) and a strong radiation source allowed us to collect high quality Mössbauer spectra also for thinnest films.

A controversial problem faced in many magnetite studies is surface termination and reconstruction. The surface structure of (001) oriented magnetite is usually discussed considering the bulk unit cell as composed of eight atomic sublayers, which contain either only tetrahedral iron atoms in A sites (so called A layer) or oxygen and octahedral B iron ions (so called B layer). The distance between A or B layers is approximately 0.2 nm, whereas the smallest interlayer spacing (A–B) is approximately 0.1 nm. Neither of the bulk terminated $Fe_3O_4(001)$ surfaces (A nor B) is charge compensated and the charge neutrality condition of the polar $Fe_3O_4(001)$ is the driving force of the reconstruction, which, although intensively studied with different methods for single crystals [17,18] as well as for epitaxial films [10,11,19–22], is still not fully understood and explained. Moreover, the valence-band spectra taken from an epitaxial film differ considerably from those of cleaved Fe_3O_4 samples and the surface spin polarization is smaller than expected [23].

In this paper we present resent results concerning $Fe_3O_4(001)$ films grown by reactive deposition on MgO(001) substrates [24,25] as well as obtained by a post-preparation oxidation of epitaxial Fe(001) films [26]. Combination of STM and CEMS studies applied in situ at ultra high vacuum conditions, resulted in the atomic scale characterization of the film surface as well as the film bulk and buried interfaces.

2. Experimental details

The experiment was performed using a multi-chamber UHV system (base pressure 1×10^{-10} mbar) which was described previously [27]. The preparation chamber contains a miniature MBE system, consisting of metal vapor sources and quartz monitors to control the evaporation rate and a four-grid LEED/AES spectrometer. The CEMS chamber is dedicated to the in situ measure-
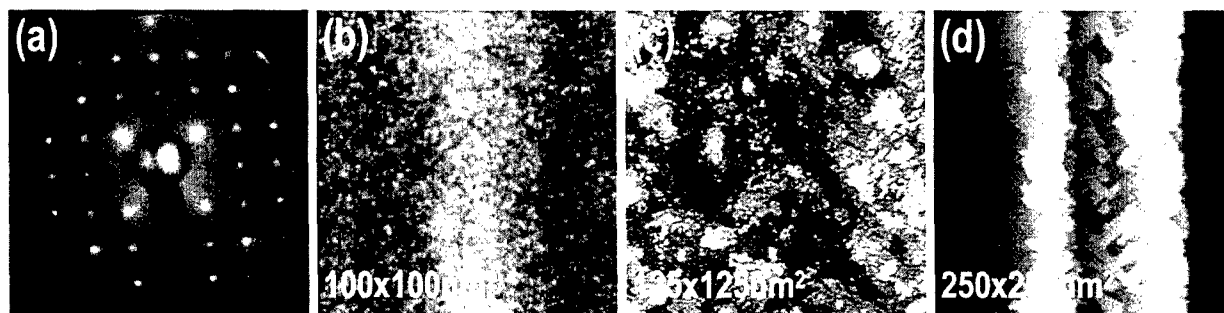
Fig. 1. (a) LEED pattern at the electron energy of 70 eV for the $(\sqrt{2} \times \sqrt{2})R45°$ reconstructed surface of the 20 nm $Fe_3O_4(001)$ film on MgO(001) and STM topographic scans: (b) for the as-deposited surface-deposition temperature 520 K, (c) after 1 h annealing at the deposition temperature and (d) after 1 h annealing at 820 K.

ments of the Mössbauer effect by detection of the conversion electrons using a large opening channeltron. The sample was mounted to a cold finger of a stationary liquid nitrogen cryostat, which allowed to perform the measurements in the temperature range between 80 K and 500 K.

A second UHV system was used for in situ STM, equipped with a similar technological facility as the one described above.

All discussed samples were prepared on MgO(001) substrates cleaved in N_2 atmosphere prior to the introduction into the UHV system. The substrates were then annealed for 1 h at 900 K in UHV and after this procedure the MgO(001) surface showed atomic cleanness and perfect structural order as checked with AES and LEED. Magnetite was grown by the Fe-vapor deposition at the rate of approximately 1 nm/min, in the presence of oxygen. Oxygen was provided, using a precision leak valve, from a nozzle placed 1 cm from the substrate to achieve a relatively high local O_2 pressure avoiding contamination of the whole chamber. For the Mössbauer experiments ^{57}Fe isotope was used. The small lattice spacing mismatch (0.3%) between magnetite and the MgO substrate in the (001)-plane provides favorable conditions for the epitaxial growth, which helps in reaching the thermodynamic equilibrium. The magnetite phase could be stabilized in a broad range of the O_2 partial pressure $(1 \times 10^{-7} \div 1 \times 10^{-6}$ hPa), as controlled by a quadrupole mass spectrometer, for the substrate held at 520 K. For all sample ranging from 500 nm down to 3 nm thickness, LEED (Fig. 1a), displayed a $(\sqrt{2} \times \sqrt{2})R45°$ reconstruction relative the primitive surface bulk unit cell of magnetite. This type of reconstruction is typical for the (001) bulk magnetite surface [17] as well as for the surface of epitaxial magnetite films on MgO(001) [19–22]. Decreasing the film thickness below 5 nm caused an increase of a diffused background accompanied by spot broadening, leaving the pattern symmetry unchanged.

Ex situ STM studies of magnetite film require ion bombardment/annealing treatment for restoring the sur-

face cleanness [19–22]. We were able to study the surfaces of the as-prepared films in situ and to examine the influence of annealing as shown in Fig. 1b–d for 20 nm films. When the films were cooled down to the room temperature immediately after the deposition is completed, the STM picture revealed grainy structures with a nanometer lateral size, which by the height analysis can be identified as monoatomic terraces spaced by approximately 0.2 nm (Fig. 1b). The overall height amplitude in the presented area was <1 nm, which means that no more than five monoatomic levels were exposed. Annealing the films for 1 h at the preparation temperature resulted in an increase of the terrace size up to several nanometers (Fig. 1c). Rising the annealing temperature up to 800 K produced large flat areas with the lateral dimensions of 20–50 nm (Fig. 1d) but AES analysis indicated the presence of magnesium, which had diffused from the substrate, as it was observed previously [28].

3. Electronic and magnetic properties vs. film thickness

Mössbauer spectra were measured in situ for the films from 430 nm down to 3 nm thickness at the temperature range between 80 and 300 K. A selection of the spectra for the 430 nm and 10 nm samples at three different temperatures is presented in Fig. 2 [24].

The 430 nm sample represents the bulk stoichiometric magnetite behavior. The hyperfine magnetic field B_{hf}, the isomer shift IS and the quadrupole splitting QS are in a good agreement with the literature values for the bulk material. The component with larger B_{hf} and smaller IS corresponds to trivalent Fe ions located at the tetrahedral A sites, while the other one is interpreted as the average signal from Fe^{3+} and Fe^{2+} ions at the octahedral B sites, seen effectively due to the electron hopping as $Fe^{2.5+}$ ions. By lowering temperature, the effect of the Verwey transition can be observed in the Mössbauer spectra. The Verwey transition, as seen by our CEMS analysis, is a multistage process. When T_V
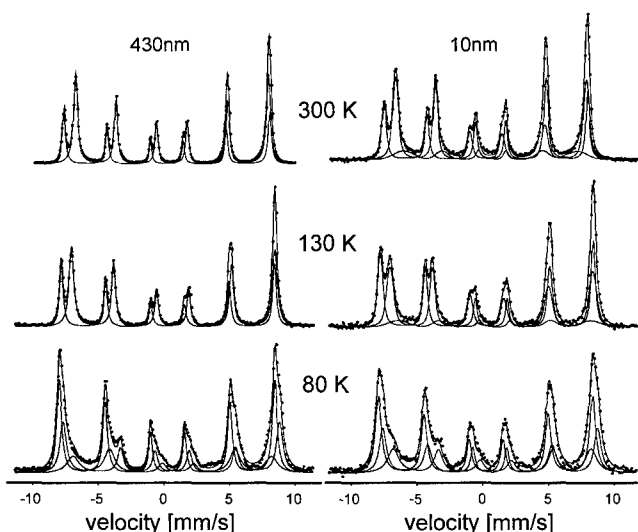
Fig. 2. Selection of CEMS results for 430 nm and 10 nm epitaxial $Fe_3O_4(001)$ films at different temperatures [24].

is approached going from high temperatures, at first the components associated with the A and B sites gradually reverse their intensity, the effect being particularly strong below 130 K for the 430 nm sample. The change of the intensity is accompanied by a broadening of the lines. This phenomenon, which is probably due to the dynamic effects connected with the electron hopping, remains not fully explained even for the bulk magnetite, indicating a highly diffuse charge dynamics. In the narrow temperature range, close to T_V, the Mössbauer spectrum undergoes drastic changes connected with the charge ordering. The electron hopping freezes, which means that the Fe^{3+} and Fe^{2+} ions at the B site differentiate in the Mössbauer spectrum. It is manifested by new components that appear in the spectrum. Eventually, in the third transition stage, which proceeds down to the lowest applied temperature (80 K), the new hyperfine pattern becomes more distinct and the lines - narrower. At 80 K, a reasonable fit with three spectral components, corresponding to Fe^{3+} at the A site, Fe^{3+} at the B site and Fe^{2+} at the B site was possible. Magnetite spectra below T_V are rather complex because of twinning, which means that there is a dipolar field distribution leading to broad and weakly resolved spectra [14]. The component corresponding to the Fe^{2+} ions at the B site is the most complex due to the characteristic high value of the quadrupole splitting QS. This is the reason why the apparent distribution of the ions at the B site between Fe^{3+} and Fe^{2+} deviates considerably from the expected 1:1 ratio.

The spectra for the 10 nm sample are similar to those for the 430 nm one (comp. Fig. 2). However, besides the slightly lowered values of B_{hf} for the component A and B, there is one remarkable difference at the room temperature. A third component with a relatively broad

distribution of B_{hf} has to be added to the fitted spectrum. We interpret this component as the one coming from the interface, where diffusion of Mg and Fe cations takes place, as suggested earlier for annealed magnetite films [28]. The contribution of the interfacial component to the spectrum reaches 15%. Taking into account that the contribution of the A site for the 10 nm spectrum remains unchanged with respect to a bulk and it amounts to 1/3, it is obvious that the interfacial component originates from the octahedral sublattice, in which the Fe ions have been replaced by Mg ones. By this assumption, from the relative area ratio of the spectral components, the thickness of the interface zone is estimated as 2.0 nm. At the low temperature (80 K), the spectral component from the Mg rich phase and the B site Fe^{2+} ions cannot be resolved due to an intricate character of the spectra below the Verwey transition. Our observation contradicts the earlier CEMS studies of the Fe_3O_4/MgO interface using ^{57}Fe probe layer [29], where no deviation from the magnetite stoichiometry was observed. However, it has to be noted that the broad interfacial component could be detected only thanks to high spectrum statistics and quality. Even more intriguing, is that the ultra thin magnetite layers in Fe_3O_4/MgO multilayers, were found to be compositionally uniform [30,31].

Around T_V, the interpretation of the Mössbauer spectra is difficult but the Verwey transition can be followed using a spectrum parameter, which is independent on the applied spectrum model. Our analysis is based on the observation of the total amplitude ratio of the outermost line groups at the positive and negative velocities. For stoichiometric magnetite, well below the Verwey transition, the '1/6 ratio' parameter (defined by the inset in Fig. 3) is very close to 1. The plots of '1/6 ratio' vs. temperature (Fig. 3) clearly reveal a complicated character of the transition reflected in the Mössbauer spectra. For the 10 nm sample the transition is much broader than for the 430 nm one. The first transition stage observed as a gradual intensity reversal
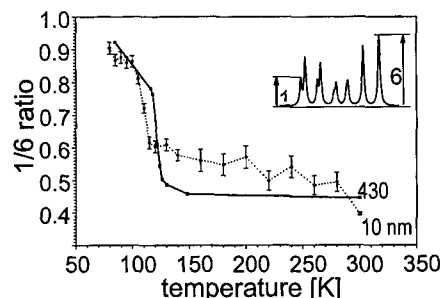

Fig. 3. '1/6 ratio' parameter plotted vs. temperature for the 430 nm (■) and the 10 nm (○) thick samples (error bars for the 430 nm sample are less than the size of points). '1/6 ratio' is defined in the inset [24].
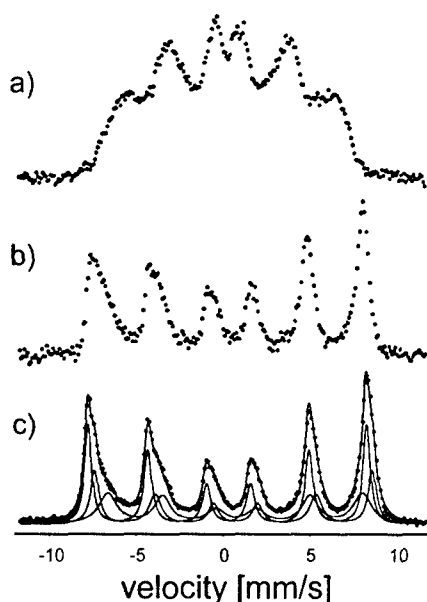
Fig. 4. CEMS spectra for the 3 nm epitaxial $Fe_3O_4(001)$ film at 300 K (a), 130 K (b) and 80 K (c) [24].

of the components A and B has its onset for the thin sample just below the room temperature, whereas for the thick sample this transition stage is nearly completely suppressed. Similarly, at low temperatures, the transition region for the thin sample is much broader than for the thick one. This is an indication that the transition may change from the first order to the second order when the sample becomes thinner. The reason of the change in the transition character may be either lattice strains due to the lattice mismatch with the substrate or the natural doping with Mg coming from the substrate.

The value of T_V is the important information source concerning the magnetite stoichiometry. T_V varies from 125 K (for δ close to 0) to approximately 100 K for highly non-stoichiometric samples ($\delta = 0.02$) [33]. From Fig. 3 T_V for the 430 nm film is estimated as 122 K indicating nearly perfect stoichiometry, whereas the 10 nm sample undergoes the transition at approximately 110 K.

The spectra for the thinnest studied sample, which was 3 nm thick, are shown in Fig. 4. At 300 K a typical relaxation character of the spectra is obvious (Fig. 4a). Similar behavior observed for magnetite films on sapphire [32] and for Fe_3O_4/MgO multilayers [34] was attributed to superparamagnetism. Superparamagnetism in ultrathin magnetite films originates from the nucleation of the Fe_3O_4 films on MgO(001) [34]. The lower symmetry of the inverse spinel structure and the larger unit cell compared to the MgO substrate mean that the magnetite islands can nucleate in eight different ways and coalescence of different islands leads to a formation of antiphase boundaries, which are a perturbation for the exchange interaction. The relaxation character of the

spectrum at room temperature does not allow to conclude about the chemical composition and the electronic properties. However, by lowering the temperature, the superparamagnetic relaxation is blocked and below 200 K the spectra reveal their static character. From low temperature measurements (Fig. 4b,c) it is clear that the 3 nm sample shows the behavior which differs considerably from the bulk magnetite-like one. The most important observation is that the spectra resemble those for magnetite below the Verwey transition, at least in the whole temperature range where the superparamagnetic relaxation is slow enough to give a static magnetic spectrum with a well-resolved hyperfine pattern, i.e. between 80 and 200 K. It could mean that the Verwey transition in the ultrathin magnetite films is shifted to higher temperatures (or completely suppressed). An alternative explanation involves formation of a magnesium rich inverse spinel, which is structurally isomorphic with magnetite and then indistinguishable by diffraction methods (LEED, RHEED or X-rays). Our films were grown at the temperature (520 K) at which, massive Mg surface diffusion through a thick film cannot be expected, but the formation of a magnesium rich spinel phase at the interface occurs as it is seen for the 10 nm sample. James et al. [35] concluded that no magnesium ferrite is formed in Fe_3O_4/MgO multilayers but the result is based on superparamagnetic spectra and in our opinion is not proved sufficiently. Summarizing, we suggest that the suppression of the Verwey transition in ultrathin magnetite films (thinner than 5 nm) originate from their chemical composition (high concentration of magnesium impurities) and that the structure and composition of ultrathin magnetite films, and at the $Fe_3O_4/$ MgO interface, differ strongly from those of a bulk. This observation remains in direct contradiction with the previous results [29–31,34,35].

4. Surface and interface seen by CEMS and STM

In magnetite films, composition inhomogeneities are expected not only at the film/substrate interface, as mentioned above but also at the surface. This problem was addressed by Fuji et al. [29] who used depth-selectivity of CEMS to probe surface layers with a sub-nanometer [57]Fe probe layer embedded in [56]Fe samples. Minor depth-dependent changes were confined to a few outermost atomic layers but the essential electronic bulk features, including a rapid electron hopping, were retained at the surface and also at the Fe_3O_4/MgO interface. This observation contrasts strongly with the scanning tunneling microscope images of a clean magnetite (001)-surface interpreted in terms of a Verwey-type charge ordering in the surface layer at room temperature [8]. A possible explanation for this discrepancy is oxidation and contamination of the magnetite surface, which is unavoidable during ex situ CEMS
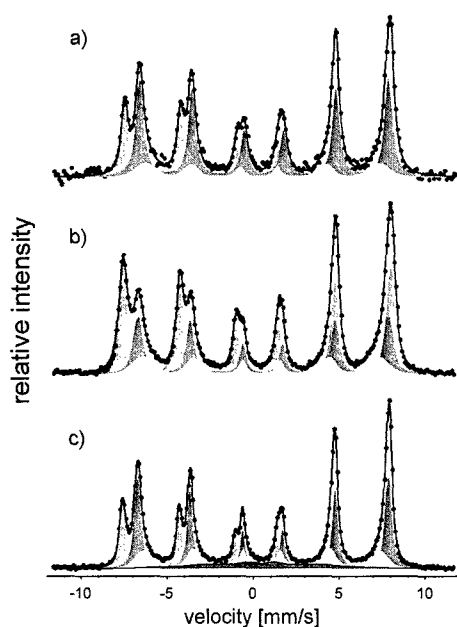
Fig. 5. Room temperature CEMS spectra of the 10 nm epitaxial magnetite film: as-grown (a), oxidized in air (b) and annealed for 1 h at 600 K at UHV (c) [25].

measurements, although, generally magnetite is thought to be stable against room temperature oxidation [32]. To clarify this problem the CEMS measurements were done for the 10 nm $Fe_3O_4(001)$ film after 1-month exposure to the atmosphere and then again at UHV condition, after being annealed in vacuum for 1 h at 600 K [25]. The measured spectra are collected in Fig. 5, together with the spectrum in the as-prepared state (Fig. 5a) repeated for a direct comparison from Fig. 2.

After an exposure of the sample to a clean air at the atmospheric pressure a drastic change in relative intensities of spectral components are clearly seen (Fig. 5b) but the hyperfine parameters of the fitted components (except the area ratio) did not change markedly. The obvious reason of the observed changes is surface oxidation. The thickness of the modified layer may be estimated based on the hypothesis of the cation vacancies formation at the octahedral sites. Assuming, for simplicity, that the oxidized phase has a homogeneous composition of γ-Fe_2O_3, the thickness of the oxidized surface layer was found to be 1.5 nm. Annealing the sample at 600 K for 1 h at UHV restored the spectra of the 'as-prepared' state (Fig. 5c). The UHV condition is strongly reducing and reverses the oxidation. Annealing also has an effect on the MgO/Fe_3O_4 interface as seen by the appearance of an additional component with a broad B_{hf} distribution at approximately 25 T. The large IS and low B_{hf} values indicate that the new component should be related to a Mg rich phase. It is formed when Fe diffuses into MgO, finally forming a $Fe_{1-x}O$ wustite-type oxide with the cubic structure of MgO [36]. For

further investigation of this process an additional 60-nm-thick sample was prepared. By increasing the sample thickness, the interdiffusion process could be studied in a broader temperature range. The final effect of the annealing cycles is shown in Fig. 6. After the last annealing cycle at 1000 K, a Mg-doped magnetite phase component and a wustite-like doublet (IS = 1.04 mm/s, QS = 0.33 mm/s) can be identified unambiguously in the Mössbauer spectrum. The deeply buried wustite layer could not be detected by other methods [37]. By comparison with the spectra of the Mg-doped magnetite single crystals [38], the average Mg concentration x in the formula $Mg_xFe_{3-x}O_4$ is estimated to be 0.10–0.15. From the intensity of the spectral components, the thickness of the wustite layer formed in the MgO substrate is found to be approximately 5 nm.

Because of the observed oxidation, surface sensitive studies of magnetite require in situ measurements. In Fig. 7 we show in situ CEMS spectra with the $^{57}Fe_3O_4$-probe layer deposited on top of 20 nm $^{56}Fe_3O_4$ films. When the probe layer is 2.4 nm thick a bulk-like magnetite CEMS spectrum is observed (Fig. 7a). For the films analyzed in Fig. 7b,c, a 0.8 nm probe layer is used to follow electronic surface properties of films displaying different surface reconstruction: ($\sqrt{2} \times \sqrt{2}$)R45° (Fig. 7b) or (1×1) (Fig. 7c). The surface structure of magnetite will be discussed in more detail below, in relation to STM measurements. Here we want only to stress the obvious difference between the both spectra. For the ($\sqrt{2} \times \sqrt{2}$)R45° reconstruction, the spectrum retained many features of bulk magnetite. The spectral components of the A and B sites can be identified unambiguously although, judging from the $Fe^{3+}/Fe^{2.5+}$ component intensity ratio, the number of the Fe ions occupying perfect octahedral sites is reduced compared with the bulk stoichiometry. The 0.8 nm probe layer containing ^{57}Fe corresponds to eight ideal atomic layers of the A- and B-type. From the intensity of the three Zeeman components, which were indispensable to fit the spectrum it could be concluded that the ^{57}Fe atoms of the probe layer form approximately three
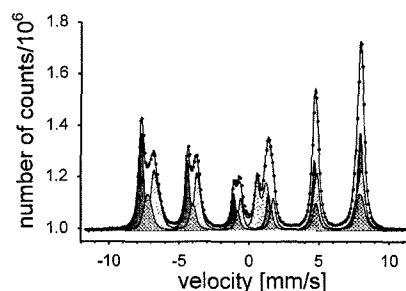

Fig. 6. CEMS spectrum after 1 h annealing cycles between 500 and 1000 K, with 100 K steps, for the 60 nm epitaxial magnetite film [25].
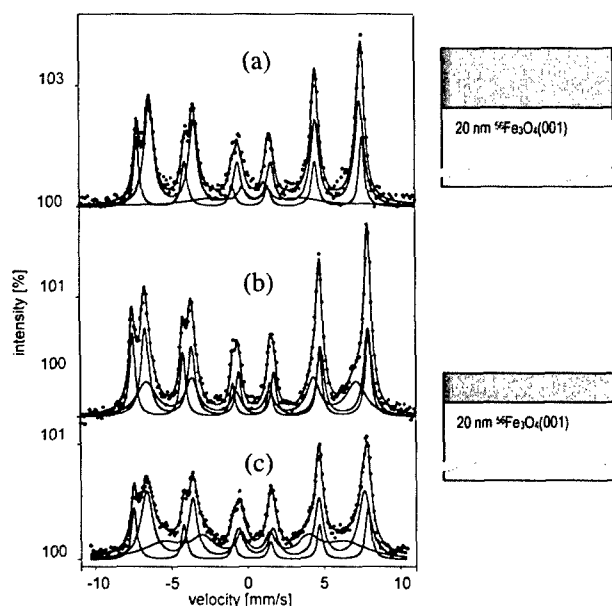
Fig. 7. Room temperature CEMS spectra of the 20 nm $^{56}Fe_3O_4(001)$ sample with $^{57}Fe_3O_4(001)$ probe layers: (a) 2.4 nm, (b) and (c) 0.8 nm with ($\sqrt{2}\times\sqrt{2}$)R45° or (1×1) reconstruction, respectively.

stoichiometric A–B layer pairs. The remaining ^{57}Fe atoms, in amount equivalent to four A or two B ideal layers, give rise to the Zeeman component with broadened lines, the reduced hyperfine magnetic field $B_{hf}=$ 42.9(5) T and the isomer shift IS=0.45(5) mm/s, which lies between the values for the A and B sites. Such component was observed also by Fuji et al. [29] and interpreted as coming from Fe^{3+} ions. From our analysis of the hyperfine parameters we favor the interpretation that it is due to all Fe ions in two or three topmost layers, which are subjected to relaxation and reconstruction.

Fig. 7c shows the CEMS spectrum for a sample displaying (1×1) reconstruction. The surface structure is very sensitive to the preparation condition and a small variation of the oxygen partial pressure during preparation, deposition temperature or post-preparation annealing may induce an irreproducible change of the surface reconstruction from ($\sqrt{2}\times\sqrt{2}$)R45° to (1×1). From the CEMS spectrum it becomes obvious that such a change is connected with a pronounced relaxation of the surface layer from the ideal spinel structure. As compared to the ($\sqrt{2}\times\sqrt{2}$)R45° reconstruction, the spectral components attributed to the surface layers are more intense and much broader. There is also a clear reduction of the Fe ion number contributing to the ideal A-type layers. It might be the indication that the (1×1) reconstruction corresponds to the surface terminated with the A-type layer.

The surface termination and interlayer relaxations of the ($\sqrt{2}\times\sqrt{2}$)R45° surface are being the subject of an intensive debate [9]. It is the most typical reconstruction

for MBE grown films monitored in situ by LEED or RHEED [19–22]. However, surprisingly, in situ diffraction experiments were never combined with in situ STM studies. It is commonly believed that autocompensation is a necessary, but insufficient, condition for the correctness of any particular surface structural model [9]. The most natural way to achieve an autocompensated $Fe_3O_4(001)$ surface that possesses the observed ($\sqrt{2}\times\sqrt{2}$)R45° symmetry is to terminate it with a half tetrahedral Fe^{3+} monolayer. However, autocompensation can also be achieved by terminating the surface with a B-type layer, in which the number of oxygen vacancies or/and the Fe^{3+} to Fe^{2+} ratio is varied. Many different reconstruction models based on A- or B-type layer termination were proposed and discussed in the literature—the most recent review can be found in the paper of Mijiritskii and Bjorma [11]. Some authors believe that both types of termination are possible, but there is the consensus that they do not occur simultaneously on one surface. Such a conclusion comes from the STM images, in which the smallest step height observed on the $Fe_3O_4(001)$ surface (see Fig. 1) is approximately 0.2 nm, which corresponds to the interplanar spacing of the A–A or B–B layers, whereas for the mixed A/B termination 0.1 nm steps are expected. Indeed, our topographic large scan STM images shown in Fig. 1 led to the same result. However, it is not necessarily true passing to the atomically resolved patterns presented in Fig. 8. The image taken at the sample bias 1 V (Fig. 8a) has a similar character to the one presented by Stanka et al. [22], which was interpreted as coming from the octahedral Fe termination with characteristic rows which are Fe ions in octahedral sites. The height histogram (below), constructed from the data in the white frame area, clearly reveals that two monoatomic terraces are spaced by 0.2 nm. Situation changes entirely for the bias voltage lowered to 0.75 V, as seen from Fig. 8b. Already, from a visual inspection, it becomes obvious that the surface structure is more complicated and diversified than it could be expected from a simple model assuming a homogenous octahedral or tetrahedral termination. The apparent step height depends on the tunneling conditions. The height histogram for the same area shows now a broad distribution without any pronounced features of steps. We were also able to demonstrate that by changing the bias to negative values the image symmetry changes completely, indicating tetrahedral termination [39]. Consequently, we postulated a mixed octahedral/tetrahedral termination, assuming that different atoms or atomic planes are imaged at different sample biases.

5. Magnetite by oxidation of Fe(001) epitaxial films

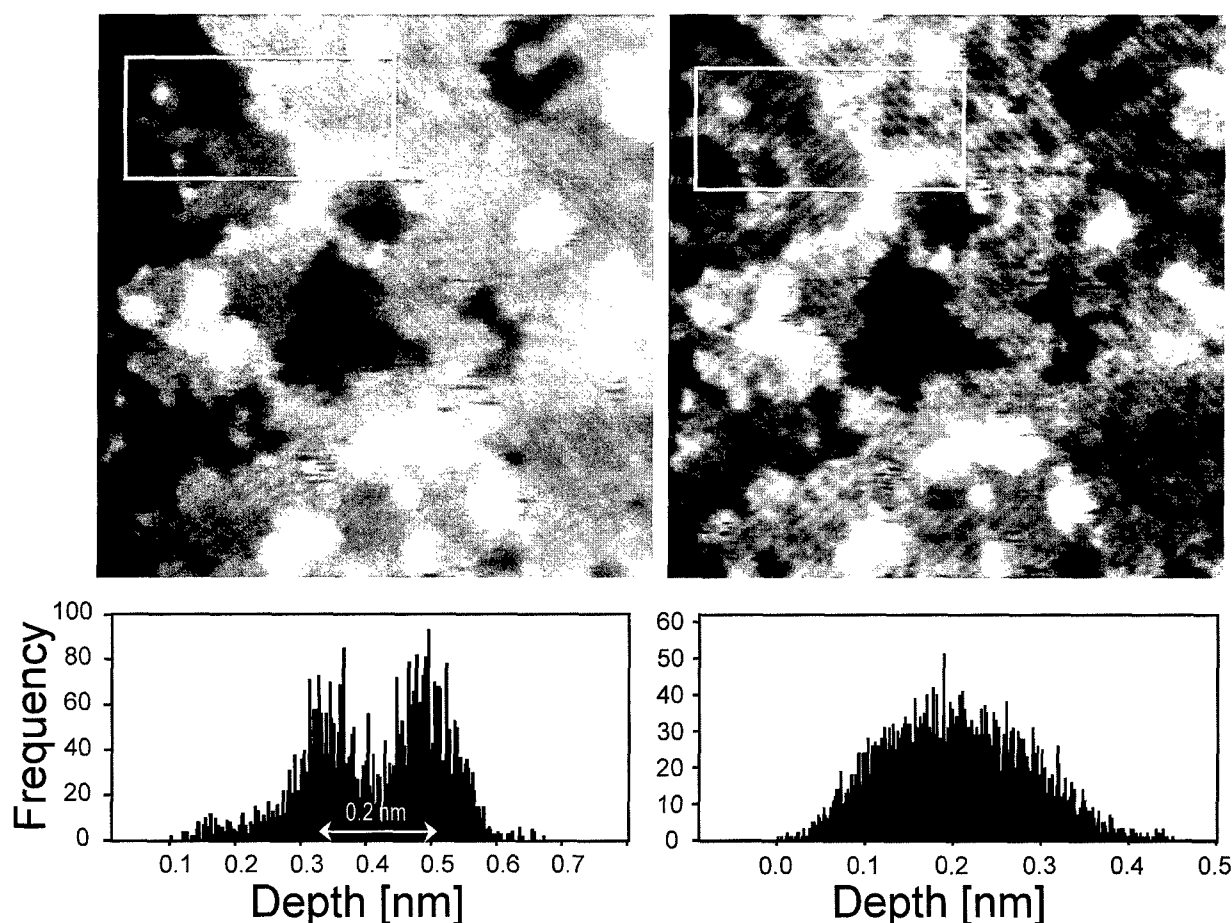Annealing improves the surface quality (lateral size of terraces) but it inevitably leads to the diffusion of

Fig. 8. Atomically resolved 30×30 nm² STM images of the 20 nm Fe₃O₄(001) film on MgO(001) taken at different sample biases: 1 V (left) and 0.75 V (right). Below: height histograms from the marked areas.

magnesium into the magnetite film. This phenomenon sets a temperature limit for the growth of Fe_3O_4(001) on MgO(001) by the reactive deposition of Fe. An alternative preparation procedure, used for the Fe_3O_4(111) growth on metallic substrates is oxidation of epitaxial ultrathin Fe films [40,41]. We have used a similar preparation technique for oxidizing an epitaxial Fe(001) film on MgO(001) [42]. To enable further studies with the Mössbauer spectroscopy, the iron isotopes [57]Fe and [56]Fe were used to enhance the surface sensitivity and a typical sample was engineered by placing the 5 nm [57]Fe probe layer on top of the 20 nm [56]Fe film. Iron was evaporated from thermal sources on polished MgO(001) substrates at an elevated temperature that was optimized for a flat growth [42]. Fe grows on MgO(001) with epitaxial relations: Fe(001)// MgO(001) and Fe[110]//MgO[100], i.e. by the 45° rotation of the (001) surface unit cell. A flat growth is reported for Fe on MgO at elevated temperatures [42] but to prevent an island-type growth nucleation should proceed at low temperature (e.g. 300 K) and then temperature can be raised gradually up to 620 K at a final thickness. Fig. 9a documents the surface topogra-

phy of the 20 nm film obtained according to the above receipt. An oxide layer was formed on the Fe(001) surface by annealing the film for 15 min at 550 K in 10^{-4} Pa O_2 partial pressure. The oxidation resulted in the formation of a new epitaxial phase observed in a LEED pattern (Fig. 9b). The pattern symmetry indicated that the layer could be a magnetite. The STM image showed distinct changes of the film topography (Fig. 9c). Small irregular grains transformed after annealing to monoatomic terraces with atomically resolved structures characteristic for magnetite [22], as shown in the inset in Fig. 9c. Unambiguous identification of the layer formed is given by a CEMS measurement shown in Fig. 10. The spectrum could be fitted with four components. Components (A) and (B) come from magnetite representing Fe ions in tetrahedral and octahedral sites, respectively. Component (M) is due to a metallic iron. Apparently, the oxidation affected only a part of the top [57]Fe layer. Component (I) comes probably from an interfacial layer formed between Fe_3O_4 and metallic iron. Neglecting differences in recoilless fractions, the thickness of the oxide layer can be estimated by comparing the relative intensity of the spectral components,
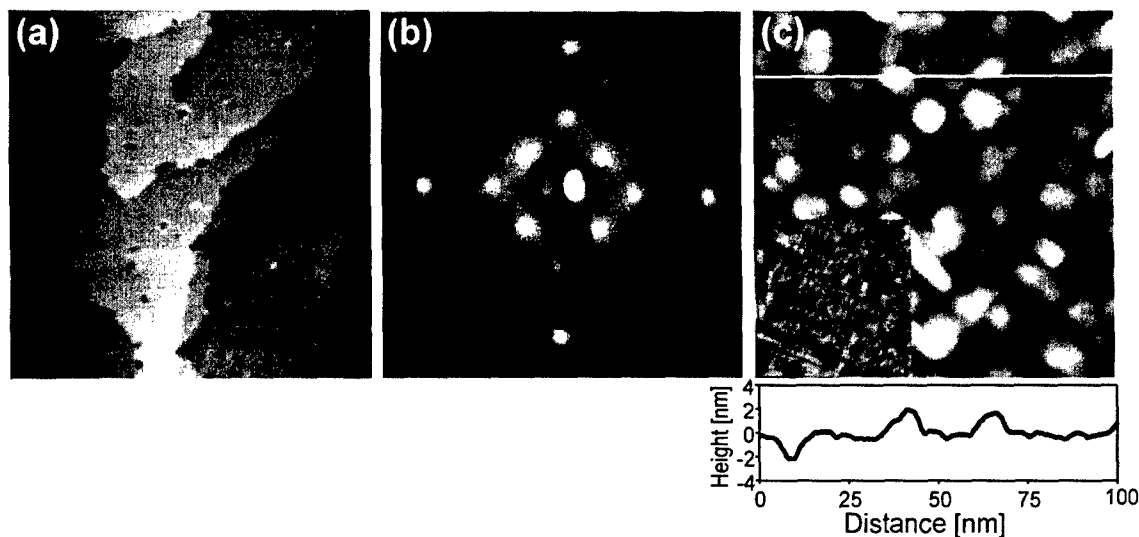
Fig. 9. Oxidized 20 nm-^{56}Fe/5 nm-^{57}Fe epitaxial film on MgO(001) as characterized by LEED and STM: (a) 100×100 nm^2 topographic STM image of the Fe(001) surface before oxidation, (b) LEED pattern at 94 eV after oxidation and (c) 100×100 nm^2 topographic STM image after oxidation. Inset on (c) shows the 12.5×12.5 nm^2 atomically resolved scan of the film annealed at 750 K.

which indicated that the magnetite layer formed on the epitaxial Fe(001) film is 3 nm thick. The Fe$_3$O$_4$(001) layer obtained in this way could be subjected to a high temperature annealing for improving the structure because the remaining Fe layer sets an effective barrier for Mg diffusion.

6. Conclusions

Highly sensitive in situ CEMS measurements gave us precise structural and magnetic characterization of epitaxial magnetite films grown on MgO(001). By lowering the film thickness down to the 10 nm range, the electronic film properties reflected in the Verwey transition are modified considerably: T_V decreases, the transition becomes broader. We attributed these changes to the MgO/Fe$_3$O$_4$ interface, at which a magnesium rich phase is postulated based on the CEMS results. The surface electronic properties seen by a probe layer

correlate with the surface reconstruction. Modifications of the surface hyperfine pattern for the $(\sqrt{2} \times \sqrt{2})R45°$ reconstruction are weaker than for the (1×1) one.

In situ STM shed some light on the surface termination of the Fe$_3$O$_4$(001) films. By the analysis of the STM images at different bias voltages, we suggest that a mixed A- and B-type termination can occur on a one surface.

Preparation of Fe$_3$O$_4$(001) films by oxidizing epitaxial Fe(001) films gives a promising perspective for growing layers with unique structural and magnetic properties.

Acknowledgments

References

[1] V.E. Henrich, P.A. Cox, The Surface Science of Metal Oxides, Cambridge University Press, Cambridge, 1993.

[2] H.H. Kung, Transition Metal Oxides: Surface Chemistry and Catalysis, Elsevier, Amsterdam, 1989.

[3] P. Marcus, V. Maurice, in: K.E. Heusler (Ed.), Passivation of Metals and Semiconductors, Trans Tech, Switzerland, 1994, p. 221.

[4] G.A. Prinz, Phys. Today 48 (1995) 58.

[5] P.J. van der Zaag, P.J.H. Bloemen, J.M. Gaines, R.M. Wolf, P.A.A. van der Heijden, R.J.M. van de Veerdonk, W.J.M. de Jonge, J. Magn. Magn. Mater. 211 (2000) 301.

[6] C.H.F. Peden, G.S. Herman, I.Z. Ismagilov, B.D. Kay, M.A. Henderson, Y.-J. Kim, S.A. Chambers, Catal. Today 51 (1999) 513.
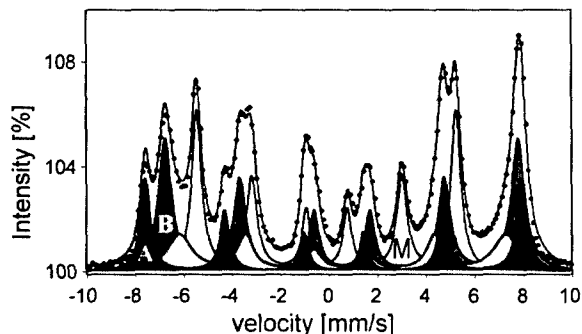

Fig. 10. In situ CEMS spectrum of the oxidized 20 nm-^{56}Fe/5 nm-^{57}Fe epitaxial film on MgO(001).

[7] U. Diebold, in: A.W. Czanderna, C.J. Powell, T.E. Madey (Eds.), Specimen Handling, Preparation, and Treatments in Surface Characterization, Kluwer Academic, New York, 1998.

[8] J.M.D. Coey, I.V. Shvets, R. Wiesendanger, H.-J. Güntherodt, J. Appl. Phys. 73 (1993) 6742.

[9] S.A. Chambers, Surf. Sci. Rep. 39 (2000) 105.

[10] F.C. Voogt, Ph.D. Thesis, Departments of Chemical Physics and Nuclear Solid State Physics, University of Groningen, Netherlands, 1998.

[11] A.V. Mijiritskii, D.O. Boerma, Surf. Sci. 486 (2001) 73.

[12] J.P. Schepherd, J.W. Koenitzer, R. Aragón, C.J. Sandberg, J.M. Honig, Phys. Rev. B 31 (1985) 1107.

[13] G.Q. Gong, A. Gupta, G. Xiao, W. Qian, V.P. Dravid, Phys. Rev. B 56 (1997) 5096.

[14] R.S. Hargrove, W. Kündig, Solid. State Commun. 8 (1970) 303.

[15] D.T. Margulies, F.T. Parker, M.L. Rudee, F.E. Spada, J.N. Chapman, P.R. Aitchison, A.E. Berkowitz, Phys. Rev. Lett. 79 (1997) 5162.

[16] J. Korecki, U. Gradmann, Phys. Rev. Lett. 55 (1985) 2491.

[17] G. Tarrach, D. Burgler, T. Schaub, R. Wiesendanger, H.-J. Güntherodt, Surf. Sci. 285 (1993) 1.

[18] C. Seoighe, J. Naumann, I.V. Shvets, Surf. Sci. 440 (1999) 116.

[19] J.M. Gaines, P.J.H. Bloemen, J.T. Kohlhepp, C.W.T. Bulle-Lieuwma, R.M. Wolf, A. Reinders, R.M. Jungblut, P.A.A. van der Heijden, J.T.W.M. van Eemeren, J. aan de Stegge, W.J.M. de Jonge, Surf. Sci. 373 (1997) 85.

[20] S.A. Chambers, S.A. Joyce, Surf. Sci. 420 (1999) 111.

[21] S.A. Chambers, S. Thevuthasan, S.A. Joyce, Surf. Sci. 450 (2000) L273.

[22] B. Stanka, W. Hebenstreit, U. Diebold, S.A. Chambers, Surf. Sci. 448 (2000) 49.

[23] H.-J. Kim, J.-H. Park, E. Vescovo, Phys. Rev. B 61 (2000) 15288.

[24] B. Handke, T. Slezak, M. Kubik, J. Korecki, J. Radioanal. Nucl. Chem. 246 (2000) 27.

[25] B. Handke, J. Haber, T. Slezak, M. Kubik, J. Korecki, Vacuum 63 (2001) 331.

[26] I. Flis-Kabulska, B. Handke, N. Spiridis, J. Haber, J. Korecki, Surf. Sci., in press.

[27] J. Korecki, M. Kubik, N. Spiridis, T. Slezak, Acta Phys. Polonica A 97 (2000) 129.

[28] J.F. Anderson, M. Kuhn, U. Diebold, K. Shaw, P. Stoyanov, D. Lind, Phys. Rev. B 56 (1997) 9902.

[29] T. Fuji, M. Takano, R. Katano, Y. Isozumi, Y. Bondo, J. Magn. Magn. Mater. 130 (1994) 267.

[30] C.L. Chang, G. Chern, Y.R. Chean, C.L. Chen, Appl. Surf. Sci. 161 (2000) 448.

[31] G.J. Strijkers, J.T. Kohlhepp, P.A.A. van der Heijden, H.J.M. de Jonge, J.M. Gaines, J. Appl. Phys. 85 (1999) 5294.

[32] T. Fuji, M. Takano, R. Katano, Y. Bondo, Y. Isozumi, J. Appl. Phys. 66 (1989) 3168.

[33] J.M. Honig, J. Alloys Comp. 229 (1995) 24.

[34] F.C. Voogt, T.T. Palstra, L. Niesen, O.C. Rogojanu, M.A. James, T. Hibma, Phys. Rev B 57 (1998) R8107.

[35] M.A. James, F.C. Voogt, L. Niesen, O.C. Rogojanu, T. Hibma, Surf. Sci. 402–404 (1998) 332.

[36] A. Perez, G. Marest, B.D. Sawicka, J.A. Sawicki, T. Tyliszczak, Phys. Rev. B 28 (1983) 1227.

[37] K.A. Shaw, E. Lochner, D.M. Lin, J. Appl. Phys. 87 (2000) 1727.

[38] J.L. Dormann, T. Merceron, P. Renaudin, V.A.M. Brabers, J. Phys. (Paris) Colloq. 41 (C1) (1980) 177.

[39] N. Spiridis, J. Korecki, in preparation.

[40] G.H. Vurens, M. Salmeron, G.A. Somorjai, Surf. Sci. 201 (1988) 128.

[41] W. Weiss, M. Ritter, Phys. Rev. B 59 (1999) 5201.

[42] S.M. Jordan, J.F. Lawler, R. Schad, H. van Kempen, J. Appl. Phys. 84 (1998) 1499.